

Introduction: The information present in the phase of gradient-echo images [1,2] has opened a new window to look at fine brain anatomy. To obtain high quality phase images [2] depicting small field perturbations produced by tissue susceptibility differences, large slowly spatially varying phase shifts due to air-tissue interfaces have to be removed. Various techniques have been proposed to fit this background field with the field generated by magnetic dipoles that either demand extra information regarding the object [3], or user input [5], or have require high number of iterations [4,6]. In this work, a fast converging method based on an approximate solution of the Matching Pursuit iterative procedure [7] is presented, which regularizes this ill-posed deconvolution problem by exploiting the spatial sparsity of the sources of the background field.

Theory & Methods: The magnetic field shift, $\delta(r)$, generated by a certain magnetic susceptibility, $\chi(r)$, can be simply described as $\delta(r)=B_0FT^{-1}(C(k)FT(\chi(r)))$, where $C(k)$ is the k-space representation of the magnetic dipole kernel. Although this linear problem, $\delta(r)=A\chi(r)$, is not invertible [4], meaningful solutions, can be obtained by simply considering $\chi(k)=0$, when $|C(k)|<t$, and $\chi(k)=\delta(k)/(B_0C(k))$, otherwise [5]. This solution is a regularized approximation of $\chi(r)=A^{-1}\delta(r)$, characterized by the threshold t . The proposed algorithm, presented in detail in Figure 1, uses this approximation to find a solution of a susceptibility distribution outside the object that explains most of the field inside.

To evaluate the performance of the method, a numerical head phantom (Matrix 256x256x128, res=1.25mm isotropic resolution) was used. Realistic magnetic susceptibilities relative to the average brain susceptibility were attributed to the different tissue types. Two fields were computed: (i) δ_{out} (Fig.2a) field generated in the brain region by the susceptibility of: non-brain tissues, bone and air; (ii) δ_{brain} (Fig.2b) field generated by the susceptibility of brain tissues and zero elsewhere;

The performance of the various filtering methods, F , was evaluated by measuring:

- fraction of δ_{brain} remaining after filtering= $1-\Sigma(|F(\delta_{brain})-\delta_{brain}|)/\Sigma|\delta_{brain}|$;
- fraction of δ_{out} removed $\Sigma(|F(\delta_{out}+\delta_{brain})-F(\delta_{brain})|)/\Sigma|\delta_{out}|$;

The performance of the proposed filtering as a function of the k-space threshold, n -threshold and down sampling level. Other filtering methods (eg. high pass filtering, polynomial fitting and conjugate gradient [4,6]) were also evaluated for comparison. Experimental data was acquire in a 7T system (Siemens, Erlangen), equipped with a birdcage RF-coil (Invivo), equipped with a multi echo GRE sequence TR=35ms, TE=3.4:8.3:32ms, Matrix=240x160x256 res=0.65 mm isotropic.

Results: Figure 2 shows that the presented algorithm outperforms polynomial fitting, high pass filtering and a conjugate gradient implementation (it was limited to 100 iterations). It is possible to observe that less regularized approximations of A^{-1} ($t=0.01$ corresponding to the top right point in all the Matching Pursuit algorithms) are superior at keeping information from δ_{brain} but fail to remove δ_{out} while more regularized approximations over-filter δ_{brain} . The number of iterations for $n>4$ was consistently under 40. Figure 3 shows that in *in vivo* brain field maps, the algorithm was successful at removing air tissue interface artifacts (nasal sinus and hear canal, black arrows in Fig. 3) and shim related contributions have been successfully removed after only 23 iterations.

Conclusions: This intuitive methodology shows great promise as a fast and robustness technique to remove background field contributions in phase imaging. Further understanding of the impact of the different parameters on the quality and speed of convergence in the presence of noise is the subject of future work. We conclude that this could be an important preprocessing tool in SWI or susceptibility mapping applications.

References & Acknowledgements [1] Rauscher et al., AJNR, 26, 736-42, 2005 [2] Duyn et al, PNAS, 104, 11796-801, 2007 [3] Neelavalli et al., JMRI, 29, 937-48, 2009 [4] Rochefort et al.MRM, 63(1), 2010;[5] Wharton et al.MRM, 2010; [6] Wharton et al., Neuroimage, 53(2), 2010; [7] Mallat et al, IEEE Trans. Signal Proc., 41, 1993; This work was supported by the Centre d'Imagerie BioMédicale (CIBM) of the UNIL, UNIGE, HUG, CHUV, EPFL and the Leenaards and Jeantet Foundations.

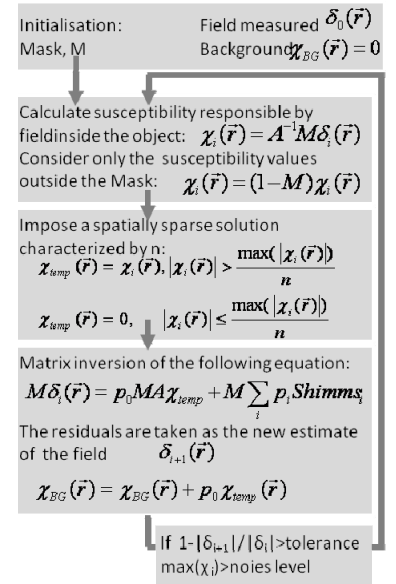


Figure 1 proposed filtering algorithm

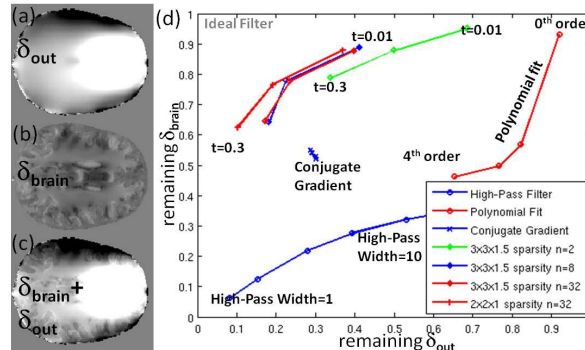


Figure 2 Field in a transverse slice generated in the brain by magnetic susceptibility: (a) outside the brain, δ_{out} ; (b) inside the brain, δ_{brain} ; (c) and their combination. (d) Plot systematizing the performance of the different background field filtering algorithms on the data shown on the left. An ideal filter would be positioned on the top left of the plot. The different curves on the top left of the graph correspond to different parameter choices for the Matching Pursuit algorithm: using different values of n ; different down sampling, Various points in the high pass filter curve, polynomial fit and conjugate gradient method correspond to the width of the Gaussian filter (1-10 pixels), order of the polynomial (0-4) and level of regularization of the CG method (1-1e10)

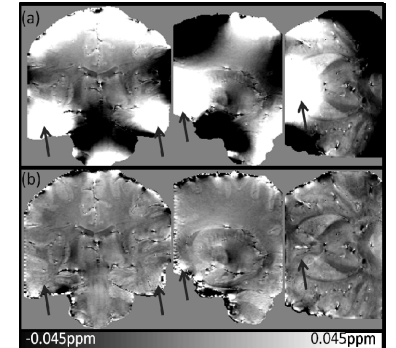


Figure 3 three orthogonal slices of partial brain field maps (a) before and (b) after filtering. For correct background field removal it was necessary to pad the FOV by a factor of 2.5, 2.5 and 6 in the x, y and z directions respectively. The calculation of the background was performed on a matrix of resolution 3x3x1.5mm³. The parameters of this specific filtering were $t=0.3$, $n=20$